Research article

"Parametric study on the age of air in a full-scale office room using perforated duct diffusers."

Peyman Raphe [a],[*], Hachimi Fellouah [a], Sébastien Poncet [a], Mohamed Ameur [b]

[a] *Department of Mechanical Engineering, Université de Sherbrooke, Sherbrooke, QC, Canada*
[b] *NAD Klima, Sherbrooke, QC, Canada*

A R T I C L E   I N F O

A B S T R A C T

Following the recent pandemic of COVID-19, scientists have made many efforts to devise a workable solution for it, worldwide. However, it was shown that the protective effect of a well-conditioning system is as high as five times in comparison to the face-covering and other proposed procedures. In this context, the age of air and the type of filtration systems in closed spaces became the critical criteria for comparing the capability of ventilation systems. In this paper, a validated numerical model for the perforated duct diffusers is used to study the behaviour of the local age of air at the full-scale office with 8 feet (2.44 [m]) height, under various initial conditions like initial velocity and air change per hour. Also, different geometries for the ducts have been investigated under the same initial condition, as well as the effect of direction, ventilation effectiveness, and flow pattern. Finally, the volume average of the age of air at different zones has been nominated to perform the sensitivity analysis of each variable based on the variation of the airflow. The results show that diffusers with vertical perforations would be more effective during the pandemic than the other types in airborne mitigation. Moreover, the highest available airflow shall be set until such time there is no windy area in the breathing zone. Within these modifications, the residence time of the infectious nuclei in the breathing zone may decrease by up to 30%.

1. Introduction

People spend more than 90 % of their time in enclosed spaces. A large fraction of that time is spent in different kinds of closed offices. That creates elevated high-air-quality ventilation systems in buildings. However, indoor air quality in the occupied zone can be dependent on many factors such as outdoor air quality, airflow rate, indoor generation of pollutants, moisture content, thermal environment, and how the air is supplied into the human-occupied zone [1]. One needs to acknowledge the importance of air distribution affecting the comfort of occupants. Heating, Ventilation, and Air Conditioning (HVAC) systems provide fresh air to the domain and recirculate the air inside the occupant zone. In other words, HVACs maintain the desired conditions by proper air distribution all around the zones. To have the most comfortable conditions in the space, different configurations, and criteria are considered. These considerations may vary from place to place in general and from zone to zone in special. The leadership in energy and environmental design (LEED) certifications and ASHRAE standards provide many rules and considerations based on statistical or experimental data for different applications and buildings [1–4]. However, local standards and frameworks have higher priority, and

---

designers have to follow them in advance. Due to the widespread of COVID-19 and the lack of information about the physics of the involved phenomena, a bunch of temporal restrictions like social distancing, regular hand washing, and face-covering have been applied to local users. Meanwhile, for long-term usage, a safer and more secure environment is associated with the modifications to operation conditions of the HVAC systems (especially the ventilation section). It was shown that the protective effect of a well-conditioning system is as high as five times in comparison to the face-covering and other proposed procedures [5]. In this context, flow physics should be investigated to omit the source of the problem. Particularly, it is inefficient to distribute the air in large spaces via a single opening, and it might be substituted by several holes or slots to have a more uniform air distribution pattern, i.e., fewer stagnant points within the room.

The virus-laden fluid particles coming from an infected patient are determined as the main source of COVID-19 transmission [6–8]. These particles are very small in size (10 [nm] - 1 [μm]) and mainly propagated via the droplets and aerosols (0.1 [μm] - 1 [mm]) of sneezing, coughing, or breathing [8]. Wells [9] first mentioned that these droplets are affected by evaporation, inertia, and gravity. So, based on the temperature and the humidity of the field, there is a critical size (50–150 [μm]) whereby the evaporation rate is higher than the settlement rate for the smaller droplets, which leads to suspended nuclei [9-10]. On top of that the average concentration of SARS-CoV-2 RNA in indoor air is higher than in the outside air, depending on the number of infected people and the ventilation system [11,12]. Alongside this statement, the concept of social distancing has been introduced to reduce the risk of contagion, especially in the indoor environment. Also, being in close interaction (less than 2 [m] away) for more than 15 [min] (900 [s]) is defined as prolonged exposure [13]. However, the sneeze large droplets may travel more than 20 ft [10,14]. In the meantime, the small particles could last for hours in the room and travel by air current in the room, but the HVAC systems could substitute them with fresh air to mitigate the contagion risk nonetheless.

The ASHRAE Design Manual for Hospitals and Clinics (DMHC) [15] defines the age of air at any arbitrary point as the elapsed time of the air after entrance. Hence, the ventilation effectiveness of HVAC systems to remove infectious particles could be compared using the mean age of air (MAA) as well as the local age of air. Since each fully mixed zone has one local mean age, one could calculate all MAA at the field (n MAA for n zones) with a single test. ASHRAE standard 129 [16] explains the test procedure, the equipment precision, and the general requirements of the step-up and step-down (decay) methods. Also, the method selected depends on the test space and the type of HVAC system. COVID-19 is a highly contagious virus and requires an extremely safe and secure test stand. Even after evaporation, the infectious particles could last for a long time over the surfaces or suspend in the air, and propagate in the room following the air current.

Designing a ventilation system, which considers all aspects of room ventilation, can only be achieved by computer modelling. In the literature [17–23], three types of methods have been used for the age of air numerical calculations in the single zone applications; one steady-state and two transient (step-down (decay) and step-up) methods. Incidentally, there are two more methods (Homogeneous Constant Emission, and Pulse Homogeneous), especially for multiple zone applications, in which the tracer gas is injected in the zone instead of a single inlet [24–27]. All methods follow the fundamental mass balance equation in the room (single or multiple zones). Variant solutions have been proposed by Afonso et al. [28], Axley and Persily [29], and Etheridge and Sanberg [30] to calculate the mean age of air. Within these proposed methods, the variation of the tracer gas concentration (usually CO_2) over time has been measured using an appropriate gas analyzer. Being feasible methods, they exhibit typically a 10% error. However, to the author's best knowledge, all of these studies are mainly concentrated on the value estimation of MAA, and there is no work on the MAA evaluation for different parameters in office rooms. Prolonged exposure elimination will not come off without prior knowledge of the room's age of air distribution patterns. The main objective of this paper is to study the effects of the different design parameters on the age of air distribution at single-zone applications. Within this parametric study, the ability of the ventilation systems to decrease the risk of any contagious nuclei with a size less than 50–150 [μm] (critical size) will be compared. Furthermore, as a secondary objective of this paper, the sensitivity of the ventilation effectiveness of the perforated duct diffusers and the uniformity of the air inside the room, as well as the breathing zone, have been analyzed.

2. Theory and mathematical model

Numerous numerical models have been proposed to calculate the local MAA to compare the performance of diffusers for deep mines [31], cleanrooms [20,32], food plants [33], extremely large open spaces [34], classical ventilated rooms [22,35,36], or comparison of ventilation systems [37–40]. Among these methods, one steady-state and two transient methods provided results with high accuracy and low computational cost. The transient methods follow the same procedure as the decay and step-up methods. However, they have a high computational cost in comparison to the steady-state method that uses the particle marker method [18,41]. So, the formulation and the concept of these three methods should be clearly understood before applying them to the numerical models.

2.1. Transient step-up method

Following the ASHRAE 129 [16] experimental step-up procedure, the contaminants or the tracer gases were born at the inlet and aged through the zones until they reached a specific location in the room. The highest age of air belongs to the particles in stagnant zones or at the farthest locations from the inlet [22]. Generally speaking, poor air distribution would increase the mean age of air, which is the main factor that represents the effectiveness of the ventilation systems.

According to the time history of the contaminant or the tracer gas and using the trapezoidal method, CFD codes calculate the MAA and air exchange efficiency of the ventilation system using Eq. (1) and unsteady approaches for all the zones.

$$\tau_i = \int_0^\infty \left(1 - \frac{c_i(t)}{c_i(\infty)}\right) dt \tag{1}$$

where τ_i is the local MAA at position i [s], $c_i(t)$ is a contaminant or tracer gas concentration at position i and time t [kg contaminant or tracer gas kg mixture^{-1}], and t is time [s].

2.2. Transient step-down (decay) method

Following the decontamination concept of the experimental decay method and prior knowledge of the concentration history, CFD codes solve Eq. (2) in the unsteady regime. It was assumed that at the start point, the tracer gas had reached a homogenous concentration in the room. The calculation continues until the room is empty of any contaminants.

$$\tau_i = \frac{1}{c_i(t_0)} \int_{t_0}^\infty c_i(t) dt \tag{2}$$

2.3. Steady-state method

Unlike transient methods, the MAA might be calculated using transport equations without prior knowledge of the tracer gas or contaminant concentration. To do so, a new set of transport equations (which is decoupled from the continuity and momentum equations) should be defined for the age of air by defining a new scalar (τ_i). So, the transport equation could be solved separately, leading to a lower computational cost. Owing to the fact that the tracer gas and the airflow should have the same behaviour in the room, ignoring the diffusion term leads to an over-predicted age of air after Gan and Awbi [18]. Abnato [36] calculated the diffusion term of this transport equation using the effective viscosity of the air (μ_{eff}), appearing in Eq. (3). One solves then a general convection-diffusion equation (Eq. 4).
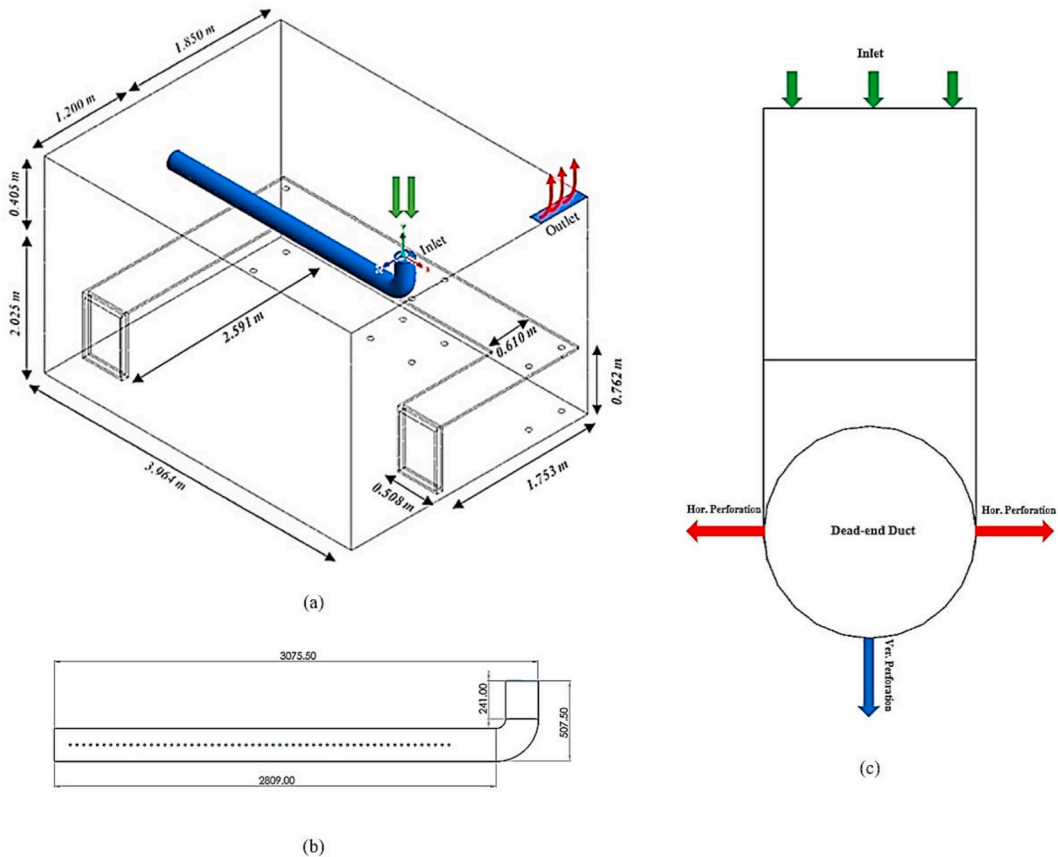
Fig. 1. (a) Small office room with installed diffuser, (b) General dimension of the duct diffusers, (c) The direction of the perforation; The red is horizontal, and the blue is vertical. (For interpretation of the references to colour in this figure legend, the reader is referred to the Web version of this article.)

$$\Gamma_{\tau_i} = 2.88 \times 10^{-5} \rho + \frac{\mu_{eff}}{0.7} \tag{3}$$

$$\nabla.(\rho \vec{v} \tau_i - \Gamma_i \nabla \tau_i) = S_{\tau_i} \, (\text{Steady-state}) \tag{4}$$

where ρ is the fluid density [kg m^{-3}], $\vec{v}$ the fluid velocity vector [m s^{-1}], Γ_{τ_i} the diffusion coefficient of the scalar τ_i and S_{τ_i} the source term of the scalar τ_i. To solve these equations, a zero gradient boundary condition at the outlet and walls as well as a zero value at the inlet and normalized source term ($S_{\tau_i} = 1$) have been suggested by many Refs. [19,20,22].

3. Numerical simulation

In the steady-state method, the age of air is a passive quantity and does not influence air distribution. Moreover, steady-state models have lower computational time in comparison to the transient models while having the same accuracy [23]. So, the age of air in this paper has been calculated using the validated steady-state models of Raphe et al. [42] for the perforated duct diffuser (PDD). Unlike the previous methods, the present model shows high accuracy for airflow distribution with less than 5% error.

It's assumed that the airflow is isothermal (295 [K]), and suspended droplet nuclei have no effect on the turbulence [43, [44]. There are no reacting elements, volatile substances, or any other sources of pollution in the room. The only mixture in the office room is the atmospheric air with constant volume and mass fractions and just the age of air and air distribution pattern in the steady-state speak of the diffuser's capability to replace the unhealthy air with fresh air. Also, the entire room boundaries (except the room inlet and outlet) are fully isolated, and the friction coefficients of the walls and duct of the diffuser are very low.

3.1. Geometry

Fig. 1-a illustrates the configuration of the small office room, while the room outlet dimension is 0.6×0.15 [m^2], and all the diffusers and the room inlet have the same radii (203 [mm]). Following the validated model [42], perforated duct diffusers were selected to perform the parametric study. These types of diffusers have horizontal or vertical equidistance perforations, and the duct is dead-end. Fig. 1-b shows the general dimensions and configuration of the fixed PDDs. From now on, if all the holes are located on both sides of the duct, it's called a horizontal perforation (shown with red arrows in Fig. 1-c). Contrary, vertical perforation ducts have holes on their bottom side (shown with blue arrows in Fig. 1-c). Also, the entire diffusers that have been used in this paper have equidistant perforations (uniform perforation), but the number of holes is double in the horizontal duct diffusers nonetheless.

3.2. Numerical method

In accordance with the reference model [42], the validated k-ε realizable turbulence model with 4.3 million unstructured linear elements is used to solve the isothermal, steady-state, fully turbulent flow. A pressure-based solver is used by considering air as an incompressible fluid with a constant density (1.225 [kg m^{-3}]), and gravity effects are accounted for (g = 9.81 [m s^{-2}]) in simulations. The governing equations are discretized by second-order upwind spatial schemes, and the SIMPLE algorithm is used to overcome the pressure-velocity coupling. The residuals level-out below 10^{-5} for the age of air, and 10^{-4} for the governing equations are also considered as convergence criteria.

3.3. Initial and boundary conditions

For the inlet velocity of 2.4 [m s^{-1}], which corresponds to 9.5 ACH, the ratio of turbulence viscosity equals 10, and 5% turbulent intensity, the simulations have been performed following the reference model [42]. Regards to the standard roughness model, walls have a no-slip shear condition, and there is no moving wall. Moreover, the room pressure is initially set to 101325 [Pa], and an outflow condition is imposed at the room outlet. There is no heat flux in the room, indeed.

4. Results and discussion

As mentioned previously, the infected droplet nuclei of diseases like COVID-19 might be suspended for hours in the room without proper conditioning. As a matter of fact, the amount of fresh air flow and its aging time at the breathing zone (BZ) are two critical parameters that indicate the cleanness of the room in the long term. ASHRAE 62.1 [1] defines the breathing zone as the region within an occupied space between planes 75 and 1800 [mm] above the floor. Furthermore, the breathing levels for the standing and sedentary occupants are 1500 [mm] and 1100 [mm] above the floor, respectively. In a nutshell, the sensitivity analysis should be performed for the distribution of the age of air at these levels as well as inlet velocity and air change per hour (ACH), which affects airflow directly (Eq. (5)).

$$\dot{V} = V.ACH = U_{inl}.A_{inl} \tag{5}$$

Where $\dot{V}$ [m^3 s^{-1}], V [m^3], U_{inl} [m s^{-1}], and A_{inl} [m^2] are air flow rate, the total volume of the room, air velocity at the inlet, and inlet area, respectively. It's noteworthy to repeat that the dimension of the room and diameter of the ducts are kept constants for all the

cases considered hereafter for the parametric study.

4.1. Effects of airflow variation

Principally, the value of the airflow depends on inlet air velocity or ACH (Eq. 6). Considering this fact, the behaviour of the key parameters in this paper was studied against the inlet air velocity variation. Later, the minimum, maximum, and mean values of the age of air in the room and breathing zone for different air flows (Table 1) were calculated. Fig. 2 shows that the general trend of the mean age of air for all the scenarios is descending with different slopes when the inlet air velocity increases. However, using the horizontal perforations leads to higher values of the MAA either in the breathing zone or room.

The maximum value of the AoA in the room shall be lower than the prolonged exposure time, assuring a safe zone for the tenants. Besides, the minimum value of the AoA in the breathing zone determines the ability of the ventilation system to replace infected nuclei with fresh air. Fig. 3 illustrates these two important parameters for different perforations altogether, making a better understanding of PDDs' performance in terms of airborne transmission. The results show that vertical perforation diffusers have provided a lower amount of AoA in general. In the meantime, using vertical perforation leads to a lower difference between the AoA of the room and the breathing zone. Statistically, using the vertical perforations at the same inlet velocity decreases the BZ's maximum AoA by 8–19%, the BZ's minimum AoA by 24–38%, and the room MAA by 4–8%. The reason for these lower values of the AoA is the higher E_z value of the vertical perforated ducts leading to higher Brownian motion of the air particles near the duct in the BZ.

Incidentally, by 40% increasing the inlet air velocity, the values of the AoA have been decreased by 25–35% approximately for all the cases. The results show that the value of the maximum AoA is more sensitive to the variation of the inlet air velocity, especially for the horizontal perforations. One reason for this fact is related to the exit jet inclination from the earlier holes. When the inlet air velocity increases, the earlier holes are subjected to the higher longitudinal component of the air velocity, which leads to exit jets that are inclined toward the end of the duct affecting the shape of air distribution at the holes' plan. Due to this fact, the horizontal velocity components of the fluid near the exit jets have different values alongside the duct, and there is a critical speed (2.4 [m s^{-1}] in Fig. 4) at which the interaction of the ceiling surface and fluid flow is sufficiently high to create a negative or low-pressure area causing the moving air mass to cling to and flow close to the ceiling surface, which is called the Coanda effect. As a result, a small stationary area is created near the diffuser whereby the maximum AoA will increase despite the increasing inlet air velocity; Which leads to bumpy curves. However, the uniformity of the AoA and air distribution shall be considered in the decision-making process for choosing the most efficient inlet air velocity. Figs. 3 and 4 show that not only the value of MAA has a descending trend with the increase of inlet air velocities, but also the discrepancy of the maximum and minimum AoA of the room has decreased. Also, for all the cases, the value of the AoA is lower than 800 [s], indicating a very short exposure time to the infected nuclei using the PDDs.

4.2. Effects of ventilation direction

Three different vertical levels are defined, namely headline (1.8 [m]), standing breathing line (1.5 [m]), and sedentary breathing line (1.1 [m] above the floor), to study the effects of key parameters. Similarly, four longitudinal levels (Planes 1 to 4, with 0.954, 1.578, 2.174, and 2.821 [m] distance from the front wall) are defined to study the variation of these parameters alongside the duct. Fig. 5 compares the distribution of the age of air at these vertical levels using horizontal and vertical perforations for five different initial velocities. As shown, the value of the age of air for the vertical perforation is lower than the horizontal perforation for each level with the same inlet velocity. This is because of the higher vertical air velocity that is injected into the breathing zone. However, higher air velocity might lead to windy zones, known as discomfort zones. So, the combination of the age of air (Figs. 5–7) and air velocity contours (similar to the proposed contours by Ref. [42]) at different levels should be considered together for the selection of the proper diffuser. The comparison of Figs. 5–7 has shown the contours of the age of air via the horizontal perforations have a more uniform distribution than the vertical ones, especially alongside the duct and near the walls, and changing the perforation pattern and directions could decrease the value of the local age of air, and the residence time of the infectious nuclei therefore, by up to 30%. Furthermore, while moving downward from the headline to the sedentary breathing line, the contours of the age of air for the horizontal perforation have lower changes. When the air velocity is in the satisfactory range (for instance, lower than 0.25 [m s^{-1}] for the cooling mode [1]), the vertical perforation has a better performance to mitigate the polluted air, especially at the standing levels.

Another important fact is by increasing the inlet air velocity, the contours of AoA alongside the duct for both scenarios find a more uniform shape (Figs. 6 and 7). Besides, the mean age of air discrepancy (Fig. 4) shows the more uniformity of the fresh air in the

Table 1
Room inlet airflow values.

$\dot{V}$ [m^3 s^{-1}]	U_{inl} [m s^{-1}]	ACH [hr^{-1}]
0.065	2	7.9
0.071	2.2	8.7
0.078	2.4	9.5
0.084	2.6	10.3
0.091	2.8	11.1

Note.
Room volume = 29.38 [m^3]; Inlet area = 0.0324 [m^{2}].
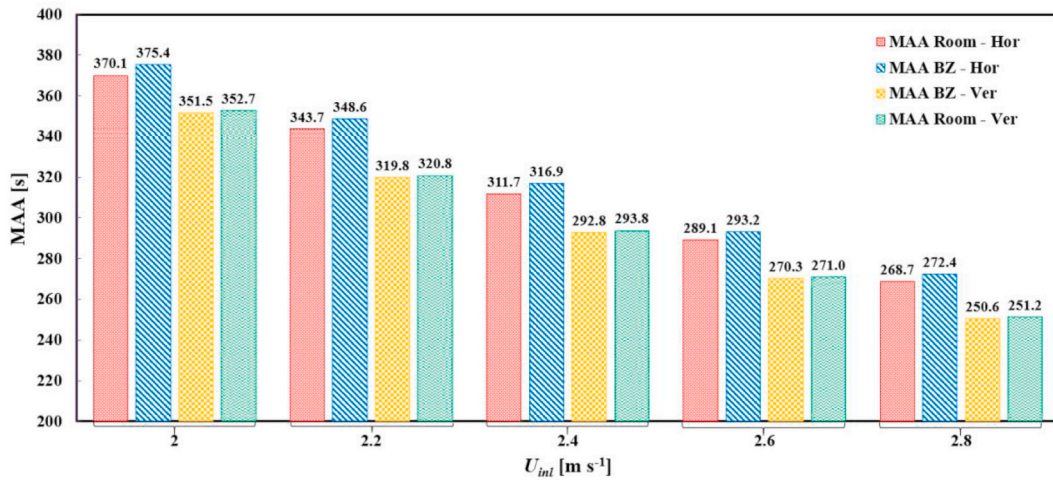
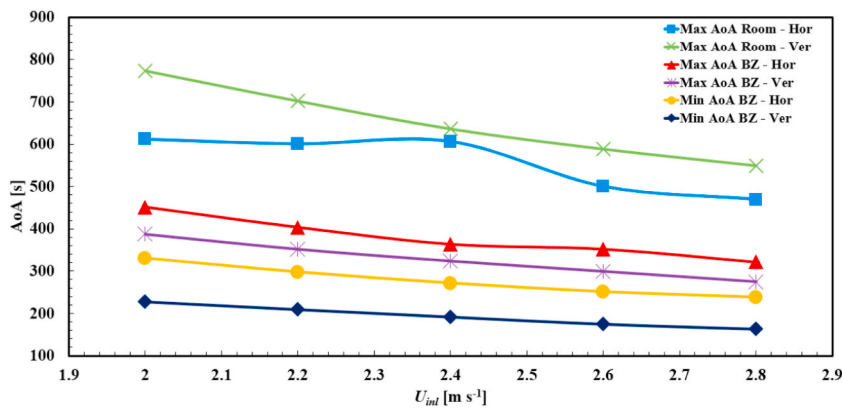**Fig. 2.** Effect of inlet air velocity on the mean age of air.

Fig. 3. Effect of inlet air velocity on the minimum and maximum age of air.
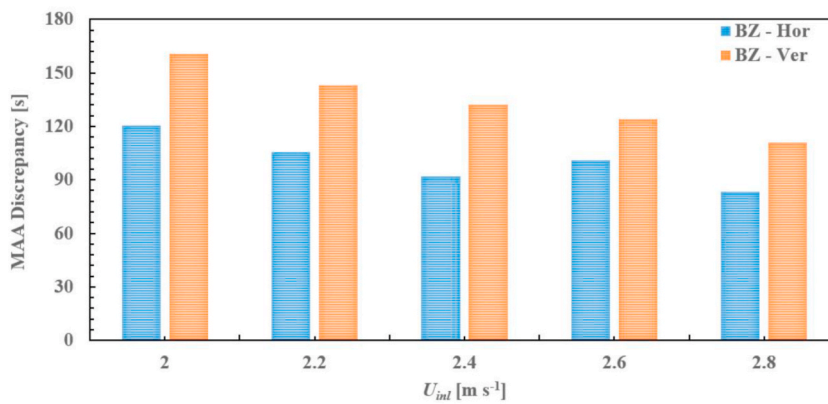

Fig. 4. Effect of inlet air velocity on the age of air discrepancy at BZ.

breathing zone using horizontal perforation, which is crucial for airborne mitigation. The presence of zones with high AoA increases the risk of infection, no matter where they are. Fig. 4 suggests that by increasing the inlet air velocity, the AoA is going to be more uniform with less difference between the upper and lower values, even though the horizontal perforation will not follow the linear trend.
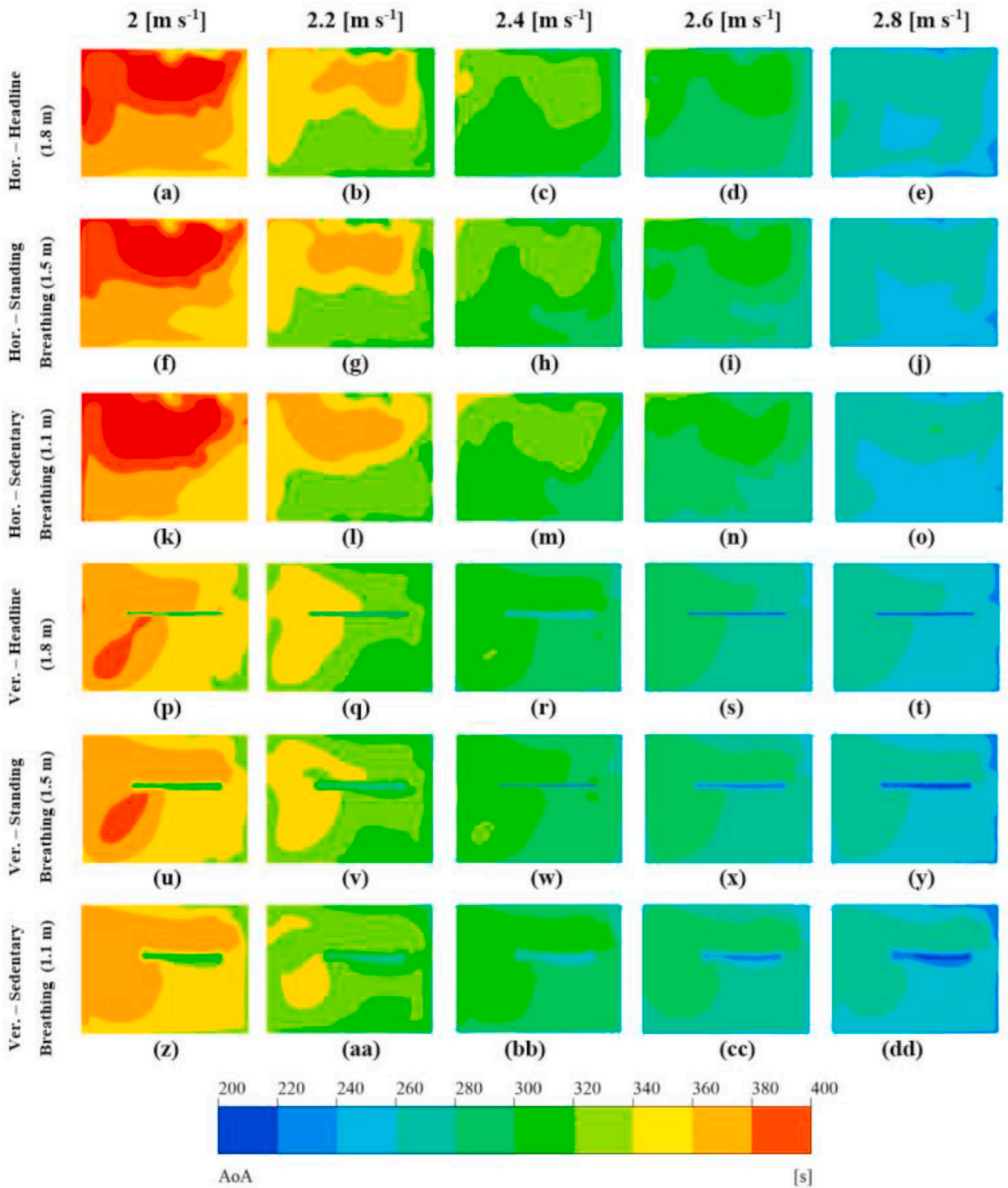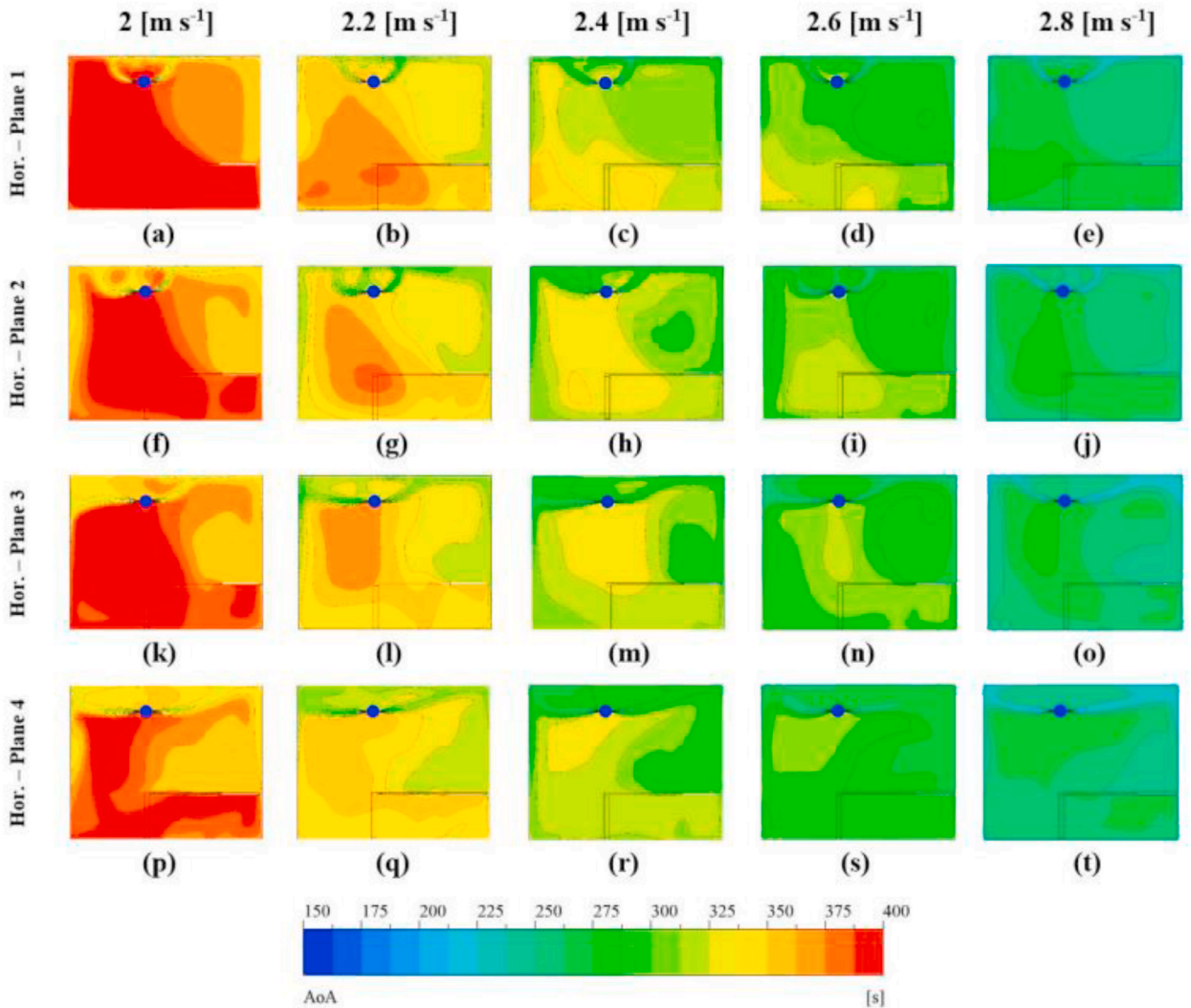
Fig. 5. AoA contours at different levels (1.8, 1.5, and 1.1 [m] above the ground) and inlet air velocities (2, 2.2, 2.4, 2.6, and 2.8 [m s^{-1}]) using horizontal and vertical perforation ducts.

4.3. Ventilation effectiveness sensitivity analysis

The elements of the air (nitrogen and oxygen) do not age inherently, and the aging indices report the molecules of the air while entering the room. Also, the fresh air is prone to be contaminated by pollutants as far as the residence time increases and getting aged.

Fig. 6. AoA contours at different Planes and inlet air velocities (2, 2.2, 2.4, 2.6, and 2.8 [m s^{-1}]) using horizontal perforation ducts.

Hence, the air exchange efficiency (η_a) has been defined to the flow pattern and compared to the performance of the diffusers. Fig. 8 illustrates the range of the air exchange efficiency for different ventilation modes in accordance with the flow pattern. The unidirectional (piston) ventilation mode has higher efficiency than the others as a result of its lower dead zones. Nevertheless, this is a theoretical value range, and it's impossible to reach the amounts near the one (very high efficiency), in reality, using the conventional diffusers. Table 2 represents the values of the air exchange efficiency and modes of ventilation for each diffuser for different airflows. Furthermore, the air change effectiveness (E) is developed to indicate the efficiency of the ventilation systems to refresh the aged air in the breathing zone. Regarding the value in Table 2, the efficiency of the diffusers with uniform horizontal perforations doesn't follow a unique pattern by the variation of the inlet velocity. In contrast, uniform vertical perforations are insensitive to the initial velocity from a ventilation effectiveness point of view. Incidentally, the vertical perforations have a higher value of η_a and E with a more uniform flow pattern in comparison to the horizontal perforations.

5. Conclusion

Highly contagious diseases like COVID-19 are easily widespread in closed spaces without or with poor ventilation. Since the small droplets evaporate soon and the droplet nuclei suspend in the room air for a long time, the aging process of the air plays a key role in lowering the contagious rate. Since the age of air inherently has integrated effects of air motion, an isothermal mode was used to investigate the ability of ventilation systems to replace infected air with fresh air, avoiding long-lasting infected particles in the room. In this paper, alongside the previous work of the authors [42], the validated numerical models are used to perform the sensitivity analysis at the isothermal mode using the k-ε Realizable turbulence model with enhanced wall treatment focusing on the age of air
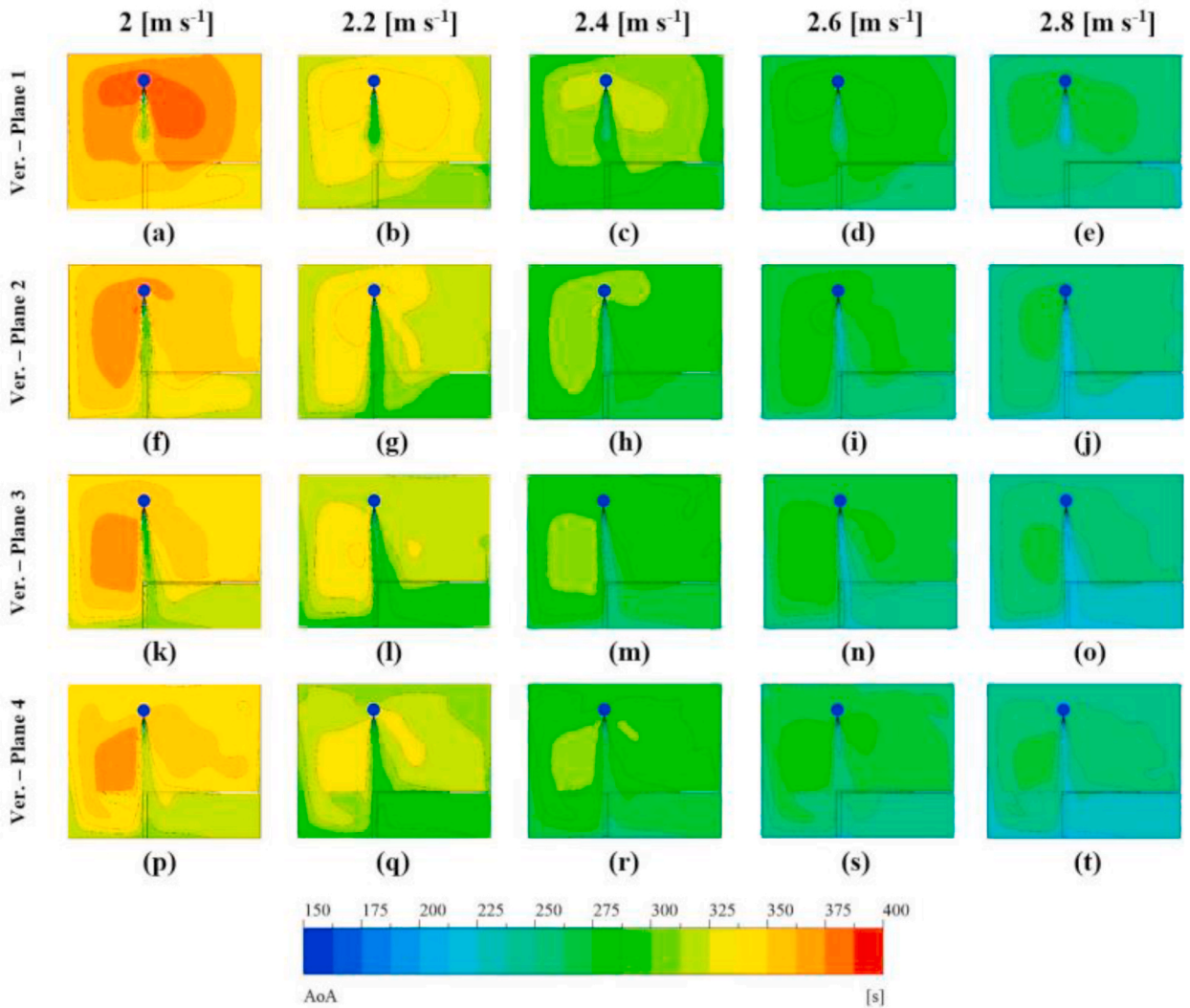
Fig. 7. AoA contours at different Planes and inlet air velocities (2, 2.2, 2.4, 2.6, and 2.8 [m s^{-1}]) using vertical perforation duct.
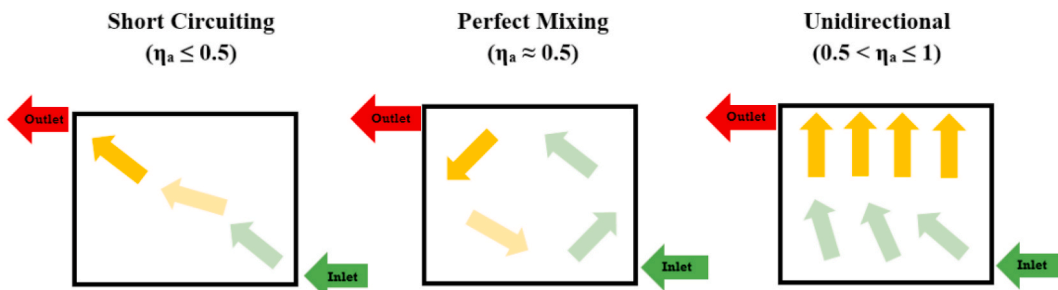

Fig. 8. Air exchange efficiency range at different modes of ventilation.

distribution. Being high induction, two types of PDDs with the same hole distance and different perforation patterns were investigated to evaluate the MAA for different parameters in office rooms, showing a 40% increase in the inlet air velocity. It lowers the AoA values by 25–35% approximately for all cases. In general, the values of the AoA and MAA for the vertical perforations (having a linear trend with the airflow variation) are lower than for the horizontal perforations under the same conditions. Furthermore, to fully understand the AoA distribution in the room, three vertical levels, namely headline (1.8 [m]), standing breathing line (1.5 [m]), and sedentary

Table 2
Comparison of the flow patterns of the PDDs.

Type of Diffuser	U_{inlet} [m s^{-1}]	Max AoA BZ [s]	MAA [s]	Nominal Time Constant [s] (AoA at room outlet, τ_a)	Air Exchange Efficiency (η_a)	Air-Change Effectiveness (E)	Flow Pattern
Uniform Horizontal Perforation	2	437.2	381.3	374.6	0.48	0.97	Short-Circuiting
	2.2	389.4	343.2	340.3	0.49	0.98	Perfect Mixing
	2.4	399.4	314.3	311.4	0.49	0.98	Perfect Mixing
	2.6	349.7	293.7	287.6	0.48	0.96	Short-Circuiting
	2.8	299.3	261.0	267.4	0.51	1.01	Unidirectional
Uniform Vertical Perforation	2	386.8	351.3	374.5	0.53	1.07	Unidirectional
	2.2	353.4	320.3	340.4	0.53	1.07	Unidirectional
	2.4	323.8	292.8	312.0	0.53	1.07	Unidirectional
	2.6	300.5	270.6	287.8	0.53	1.07	Unidirectional
	2.8	275.4	251.5	267.4	0.53	1.07	Unidirectional

Note: Uniform horizontal perforations create perfect mixing, while uniform vertical ones have a unidirectional flow pattern.

breathing line (1.1 [m] above the floor) as well as four longitudinal levels (planes 1 to 4, with 0.954, 1.578, 2.174, and 2.821 [m] distance from the front wall) have been defined. The AoA contours of these levels acknowledged the higher performance of the vertical perforation diffusers to mitigate airborne transmission in the room. In conclusion, during the pandemic, diffusers with vertical perforation would be more effective than the other type in terms of renewing the contaminated air. Though the highest available airflow shall be set until such time there is no windy area in the breathing zone. Moreover, the results indicate that uniform horizontal perforations create perfect mixing, while uniform vertical ones have a unidirectional flow pattern. As a result, uniform vertical perforations take advantage of higher ventilation effectiveness with lower energy consumption.

Declaration of competing interest

There is no conflict of interest.

Acknowledgment

Nomenclature

Abbreviations Full Name

AOA	Age of air
ASHRAE	American society of heating, refrigerating and air-conditioning engineers
CFD	Computational fluid dynamics
HVAC	Heating, ventilation, and air conditioning
ISO	International organization for standardization
MAA	The mean age of air
PDD	Perforated duct diffuser
SIMPLE	Semi-implicit method for pressure-linked equations

Symbols Name SI Unit

ACH	Air change per hour hr^{-1}
A_{inl}	Inlet area, m^2
C	Contaminant or tracer gas concentration, -
E_z	Zone air-change effectiveness, ~
Re	Reynolds number, -
S_{τ_i}	Source term of the scalar τ, -
U_{inl}	Air velocity at the inlet, m s^{-1}
V	The total volume of the room, m^3
$\dot{V}$	Air flow rate, m^3 s^{-1}

Greek Letter Name SI Unit

Γ_{τ_i}	Diffusion coefficient of the scalar τ_i, -
η_a	Air exchange efficiency, -

μ_{eff}	Effective viscosity of air, kg m^{-3}
v	Fluid velocity magnitude, m s^{-1}
ρ	Fluid density, kg m^{-3}
τ_a	Age of air at room outlet, s

References

[1] ANSI/ASHRAE Standard 62.1, Ventilation for Acceptable Indoor Air Quality, 2016.

[2] U.S. Green Building Council, LEED Reference Guide for Green Building Design and Construction, 2013. USA.

[3] U.S. Green Building Council, LEED Reference Guide for Green Building Operations and Maintenance, 2013. USA.

[4] ISO 14001:2015, Environmental Management Systems-Requirements with Guidance for Use, 2015.

[5] D. Srikrishna, A room, a bar and a classroom: how the coronavirus is spread through the air depends on heavily mask filtration efficiency? medRxiv 20227710 (2020).

[6] S. Asadi, N. Bouvier, A. Wexler, W. Ristenpart, The coronavirus pandemic and aerosols: does COVID-19 transmit via expiratory particles? Journal of Aerosol Science and Technology 54 (6) (2020) 635–638.

[7] L. Bourouiba, Turbulent gas clouds and respiratory pathogen emissions: potential implications for reducing transmission of COVID-19, J. Am. Med. Assoc. 323 (18) (2020) 1837–1838.

[8] R. Mittal, R. Ni, J. Seo, The flow physics of COVID-19, J. Fluid Mech. 894 (F2) (2020).

[9] W. Wells, Airborne contagion and air hygiene: an ecological study of droplet infections, J. Am. Med. Assoc. 159 (1) (1955), 90-90.

[10] X. Xie, Y. Li, A. Chwang, P. Ho, W. Seto, How far droplets can move in indoor environments - revisiting the wells evaporation-falling curve, Indoor Air 17 (3) (2007) 211–225.

[11] A. Dinoi, M. Feltracco, D. Chirizzi, S. Trabucco, M. Conte, E. Gregoris, E. Barbaro, G. Bella, G. Ciccarese, F. Belosi, G. Salandra, A. Gambaro, D. Contini, A review on measurements of SARS-CoV-2 genetic material in air in outdoor and indoor environments: implication for airborne transmission, Sci. Total Environ. 809 (2022).

[12] M. Conte, M. Feltracco, D. Chirizzi, S. Trabucco, A. Dinoi, E. Gregoris, E. Barbaro, G. Bella, G. Ciccarese, F. Belosi, G. Salandra, A. Gambaro, D. Contini, Airborne concentrations of SARS-CoV-2 in indoor community environments in Italy, Environ. Sci. Pollut. Control Ser. 29 (2022) 13905–13916.

[13] Public Health Agency of Canada, Updated Public Health Management of Cases and Contacts Associated with Coronavirus Disease 2019, 2020 [Available at: https://www.canada.ca/en/public-health/services/diseases/2019-novel-coronavirus-infection/health-professionals/interim-guidance-cases-contacts.html].

[14] L. Bourouiba, E. Dehandschoewercker, J. Bush, Violent expiratory events: on coughing and sneezing, J. Fluid Mech. 745 (2014) 537–563.

[15] ASHRAE Standard, HVAC Design Manual for Hospitals and Clinics, 2013.

[16] ANSI/ASHRAE Standard 129-1997 (RA-2002), Measuring Air-Change Effectiveness, 2002.

[17] C.A. Roulet, P. Cretton, Field comparison of age of air measurement techniques, Roomvent 92 (1992) 213–229.

[18] G. Gan, H.B. Awbi, Numerical prediction of the age of air in ventilated rooms, in: Proceedings Of 4th International Conference On Air Distribution In Rooms, Krakow, Poland, 1994.

[19] M. Bartak, I. Beausoleil-Morrison, J.A. Clarke, J. Denev, F. Drkal, M. Lain, I.A. Macdonald, A. Melikov, Z. Popiolek, P. Stankov, Integrating CFD and building simulation, Build. Environ. 37 (2002) 865–871.

[20] S.C. Hu, Y.K. Chuah, Deterministic simulation and assessment of air recirculation performance of unidirectional-flow cleanrooms that incorporate age of air concept, Build. Environ. 38 (2003) 563–570.

[21] J. Abanto, D. Barrero, M. Reggioa, B. Ozell, Airflow modeling in a computer room, Build. Environ. 39 (2004) 1393–1402.

[22] Z. Lin, T.T. Chow, K.F. Fong, C.F. Tsang, Q. Wang, Comparison of performances of displacement and mixing ventilations. Part II: indoor air quality, Int. J. Refrig. 28 (2005) 288–305.

[23] V. Chanteloup, P.S. Mirade, Computational fluid dynamics (CFD) modelling of local mean age of air distribution in forced-ventilation food plants, J. Food Eng. 90 (2009) 90–103.

[24] H. Stymne, C. Boman, Measurement of ventilation and air distribution using the homogeneous emission technique - a validation, in: Healthy Buildings 94, Proceedings of the 3rd International Conference, Budapest, Hungary, vol. 2, 1994, pp. 539–544.

[25] Nordtest, Ventilation: Local Mean Age of Air - Homogeneous Emission Techniques, 1997. Nordtest Method NT VVS 118, Nordtest, Finland.

[26] H. Stymne, C. Boman, The principles of a homogenous tracer Pulse technique for measurement of ventilation and air distributions in buildings, in: Proceedings of 19th AIVC Conference, Oslo, Norway, 1998.

[27] H. Stymne, P. Hansson, C. Boman, Experimental testing of a homogeneous tracer Pulse technique for measurement of ventilation and air distribution in buildings, in: Proceedings of 21st AIVC Conference, The Hague, Netherlands, 2000.

[28] C. Afonso, E. Maldonado, E. Skåret, A single tracer-gas method to characterize multi-room air exchanges, Energy Build. 9 (1986) 273–280.

[29] J. Axley, A. Persily, Integral mass balances and Pulse injection tracer techniques, in: Proceedings of 9th AIVC Conference, Gent, Belgium, vol. 1, 1988, pp. 125–157.

[30] D. Etheridge, M. Sandberg, Building Ventilation Theory and Measurement, John Wiley and Sons Ltd, Chichester, England, 1996.

[31] M. Parra, J. Villafruela, F. Castro, C. Méndez, Numerical and experimental analysis of different ventilation systems in deep mines, Build. Environ. 41 (2006) 8–93.

[32] C. Méndez, J. San José, J. Villafruela, F. Castro, Optimization of a hospital room by means of CFD for more efficient ventilation, Energy Build. 40 (2008) 849–854.

[33] O. Rouaud, M. Havet, Numerical investigation on the efficiency of transient contaminant removal from A food processing clean room using ventilation effectiveness concepts, J. Food Eng. 68 (2005) 163–174.

[34] J. Shen, L. Haas, Calculating age and residence time in the tidal york river using three-dimensional model experiments, Estuar. Coast Shelf Sci. 61 (2004) 449–461.

[35] P. Stankov, CFD prediction of air flow in A ventilated room as A tool for emerging design, Journal of Theoretical and Applied Mathematics 29 (2) (1999) 101–112.

[36] J. Abanto, D. Barrero, M. Reggio, B. Ozell, Airflow modelling in a computer room, Build. Environ. 39 (2004) 1393–1402.

[37] A. Roos, The air exchange efficiency of the desk displacement ventilation concept: theory, measurements and simulations, in: Proceedings of the 6th International Conference on Air Distribution in Rooms, Stockholm, Sweden, 1998.

[38] S. Hu, J. Barber, Y. Chuah, A CFD study for cold air distribution systems, in: Proceedings of the 1999, ASHRAE Winter Meeting, Chicago, USA, 1999.

[39] H. Chang, S. Kato, T. Chikamoto, Room air distribution and indoor air quality of hybrid air conditioning system based on natural and mechanical ventilation in an office, Int. J. Vent. 2 (1) (2003) 65–75.

[40] K. Noh, C. Han, M. Oh, Effect of the airflow rate of a ceiling type air-conditioner on ventilation effectiveness in A lecture room, Int. J. Refrig. 31 (2008) 180–188.

[41] Y. Li, L. Fuchs, S. Holmberg, Methods for predicting air change efficiency, in: Proceedings of the 3rd International Conference on Air Distribution in Rooms, Aalborg, Denmark, 1992.

[42] P. Raphe, H. Fellouah, S. Poncet, M. Ameur, Ventilation effectiveness of uniform and non-uniform perforated duct diffusers at office room, Build. Environ. 204 (2021) 108–118.

[43] S. Elghobashi, On predicting particle-laden turbulent flows, Appl. Sci. Res. 52 (1994) 309–329.

[44] D. Ting, Ventilation and airflow in buildings: methods for diagnosis and evaluation, Int. J. Environ. Stud. 65 (4) (2008) 627–628.